ELSEVIER

PII: S0032-3861(97)10070-2

Polymer Vol. 39 No. 15, pp. 3479–3489, 1998

0032-3861/98/$19.00+0.00

Effect of polyester side-chains on the phase segregation of polyurethanes using small-angle X-ray scattering

S. L. Chang[a], T. L. Yu[b,*], C. C. Huang[a], W. C. Chen[b], K. Linliu[c] and T. L. Lin[d]

[a]*Department of Nuclear Science, National Tsing Hua University, Hsinchu, Taiwan 30043*

[b]*Department of Chemical Engineering, Yuan Ze Institute of Technology, Taoyuan, Nei-Li, Taiwan 32026*

[c]*Department of Advanced Modules, Vanguard International Semiconductor Corp. 123, Park Ave-3rd, Science-Based Industrial Park, Hsinchu, Taiwan 30077*

[d]*Department of Nuclear Engineering and Engineering Physics, National Tsing Hua University, Hsinchu, Taiwan 30043*

(Received 24 April 1997; revised 18 August 1997; accepted 28 August 1997)

Small-angle X-ray scattering and differential scanning calorimetry were used to study the morphology in segmented polyester-based polyurethanes with 4,4′-methylene bis(phenyl isocyanate) and butanediol as hard segment. The polyesters with various mole ratios of $-CH_3$ side chain were synthesized from adipic acid and glycols which were mixtures of various mole ratios of hexanediol and 1,2-propanediol. The effect of $-CH_3$ side-chain content in polyesters on the phase segregation of soft- and hard-segments of polyurethanes at two annealing temperatures, i.e. 25 and 87°C, was observed. © 1998 Elsevier Science Ltd. All rights reserved.

(Keywords: polyurethane; d.s.c.; SAXS)

INTRODUCTION

The segmented polyester-based urethanes are thermoplastic elastomers with high elongation characteristics, along with typical properties of plastics such as modulus, strength and processability. It is generally agreed that the unique mechanical properties of polyurethanes, compared with other types of elastomer, are predominantly the result of a two-phase morphology of soft and hard segments[1,2]. The polyester-based urethanes consists of an aromatic diisocyanate with a glycol chain extender as the hard segment and a low molecular weight polyester as the soft segment. They are considered to be linear segmented block copolymers, made up of alternating hard and soft block segments. Compositional variables and processing conditions are known to affect the degree of phase segregation, phase mixing, hard segment domain organization, and subsequent polyurethane properties[2–4]. Depending on the relative incompatibility of hard and soft segments, phase segregation will occur during processing and post cure annealing with the hard domains acting as physical crosslinks. The effects of polyurethane composition and structure on the resultant properties have been investigated by several researchers[5–32]. These studies have been concentrated on the model compounds based on aromatic diisocyanates, such as toluene diisocyanate[5–7] or diphenyl methane diisocyanate (MDI)[5–9]. The phase segregation of hard and soft segment domains has been demonstrated by small- and wide-angle X-ray scattering[10–21], differential scanning calorimetry (d.s.c.)[10–25], infrared spectroscopy[25–30] and microscopy[17,31,32], small-angle laser light scattering[17] and dynamic mechanic thermal analysis[19].

In this work, the soft segment polyester-diols were synthesized from adipic acid with glycols which had various mole ratios of 1,2-propanediol and hexanediol. 1,2-Propanediol provided $-CH_3$ side chains in the polyester soft segment. The effect of the concentration of polyester $-CH_3$ side chains on the hard and soft segment segregation after annealing at 25 and 87°C was investigated by d.s.c. and small-angle X-ray scattering (SAXS).

EXPERIMENTAL

Polyester diol

Polyesters were synthesized by a conventional method from 1,2-propanediol, hexanediol, and adipic acid (Riedel–de Haen Co.) with an OH/COOH mole ratio of 1.18/1 under nitrogen atmosphere. The chemical compositions of five polyesters are listed in *Table 1*. 1,2-Propanediol was first reacted with adipic acid, for which the reaction temperature was increased by stepwise control as follows: 140°C/1 h, 150°C/1 h, 16°C/1 h and 170°C/1 h. The reaction mixture was then cooled to 90°C and mixed with hexanediol. After mixing, the reaction temperature was increased to 140°C. Then the reaction temperature was further increased by stepwise control as follows: 140°C/1 h, 160°C/2 h, 180°C/2 h, 200°C/4 h. The acid values of the final polyesters are listed in *Table 1*. Thus, primary –OH terminal ends were obtained for all of the polyesters, except for polyester-5 which had terminal ends with a secondary –OH group. The

* To whom correspondence should be addressed

Table 1 Chemical composition and molecular weight of polyesters

Sample	1	2	3	4	5
Adipic acid/mol	1.000	1.000	1.000	1.000	1.000
1,2-Propanediol/mol	—	0.452	0.590	0.728	1.180
Hexanediol/mol	1.180	0.728	0.590	0.452	—
Acid value/mg KOH g^{-1}	3.60	3.81	3.22	3.80	3.20
M_n	2155	2075	2500	2075	2500
M_w/M_n	1.82	1.76	1.80	1.80	1.96

Table 2 Chemical compositions of polyurethanes

Polyurethane[a]	Polyester/mol	MDI/mol	Butanediol/mol	Soft segment content/wt%
PU-1	0.326	2.1	1.673	51.0
PU-2	0.339	2.1	1.661	51.0
PU-3	0.283	2.1	1.716	51.0
PU-4	0.339	2.1	1.661	51.0
PU-4	0.283	2.1	1.716	51.0

[a] The polyurethanes were synthesized from the polyesters which have the same designated numbers as shown in *Table 1*

molecular weight distributions were determined by g.p.c. (Waters model 746 with μ-styragel columns of pore sizes of 500 Å, 10^3 Å, and 10^4 Å and an RI detector) at 25°C. Tetrahydrofuran (Merck Co.) was used as the mobile phase, and narrow MWD polystyrene standards (Aldrich Chemical Co.) were used for linear calibration. The M_n and M_w of these polyesters are also listed in *Table 1*.

Polyurethanes

The polyester-diols, synthesized as described above, were used to synthesize polyurethanes with MDI (Tokyo Kasei Kogyo Co.) as a diisocyanate compound and 1,4-butanediol (Riedel–de Haen Co.) as a chain extender by a prepolymerization method. The chemical compositions of these polyurethanes are shown in *Table 2*. Thus the polyurethanes consisted of polyester soft segments with various concentrations of $-CH_3$ side chains. Polyester-diol was first reacted with diisocyanate at 90–100°C for 1 h in *N,N*-dimethyl formamide (DMF, Merck Co.). The prepolymer was then reacted with 1,4-butanediol at 90–100°C for another hour in DMF. The final polymer was then precipitated from methanol and the residual solvent was removed under vacuum at 60°C for 24 h. The polymer was then compression moulded on a press at 175°C for 10 min followed by cooling at ambient temperature and environment. Before polymerization, polyester was distilled at 90°C under vacuum for 2 h to remove moisture. 1,4-Butanediol and DMF were treated with molecular sieve (Merck, pore size 0.4 nm) drying agent. MDI was used as-received without further purification. The final polyurethane product contained 51.0 wt% of polyesters.

D.s.c.

D.s.c. measurements were carried out on a Du Pont 910 DSC. The heating rate was 10°C min^{-1} for the temperature range −100–240°C. The size of samples was around 10 mg for all measurements. Temperature calibration was done with a multiple indium–lead–nickel standard, using an indium standard for heat flow calibration.

SAXS

SAXS measurements were performed with a pinhole collimated X-ray camera. The radiation source was a Rigaku 18 kW rotating anode generator with Cu target, to be operated at 100 mA and 40 keV (installed at the Department of Nuclear Engineering and Engineering Physics, National Tsing Hua University, Taiwan). A three-pinhole system was used to collimate the X-ray beams along with a graphite monochromator to control the incident X-ray beams on the sample. The scattered intensity was detected by a two-dimensional multi-wire detector (Oak Ridge Detector Laboratory, Inc.) with 256 × 256 channels for 20 cm × 20 cm active area (1 mm between each pixel). The sample to detector distance was 400 cm. All data were corrected for background (dark current) and the sensitivity of each pixel in the area detector.

RESULTS AND DISCUSSION

D.s.c. study

Polyurethanes annealed under two different conditions were studied herein. One series of polyurethanes was annealed at room temperature for at least 1 week. The samples were quenched to −80°C with liquid nitrogen before d.s.c. measurements. The other series of polyurethanes was the same samples used in previous series, which were annealed at room temperature for 1 week followed by annealing at 87°C for 1 h and then quenched to −80°C before d.s.c. measurements. The d.s.c. curves of polyurethanes annealed at room temperature are shown in *Figure 1*. The positions of the d.s.c. endotherms and thermal transitions are listed in *Table 3*, in which the uncertainty associated with each temperature is approximately ± 2°C. Four temperature regions were observed for d.s.c. thermal transitions and endotherms.

The soft segment glass transition temperature T_{g1}, a second-order transition, appears in the region of −40 to −18°C. The T_{g1} value can be used as an indicator of relative purity of the soft segment region. The more the soft segment domains are contaminated with the dissolved hard segments of high glass transition temperature, the higher is the polyester domain T_{g1}. The extent of hard segment/soft segment mixing will depend on the overall hard segment content, both segment lengths, the mutual affinity between segments, hydrogen bonding of urethane linkages and

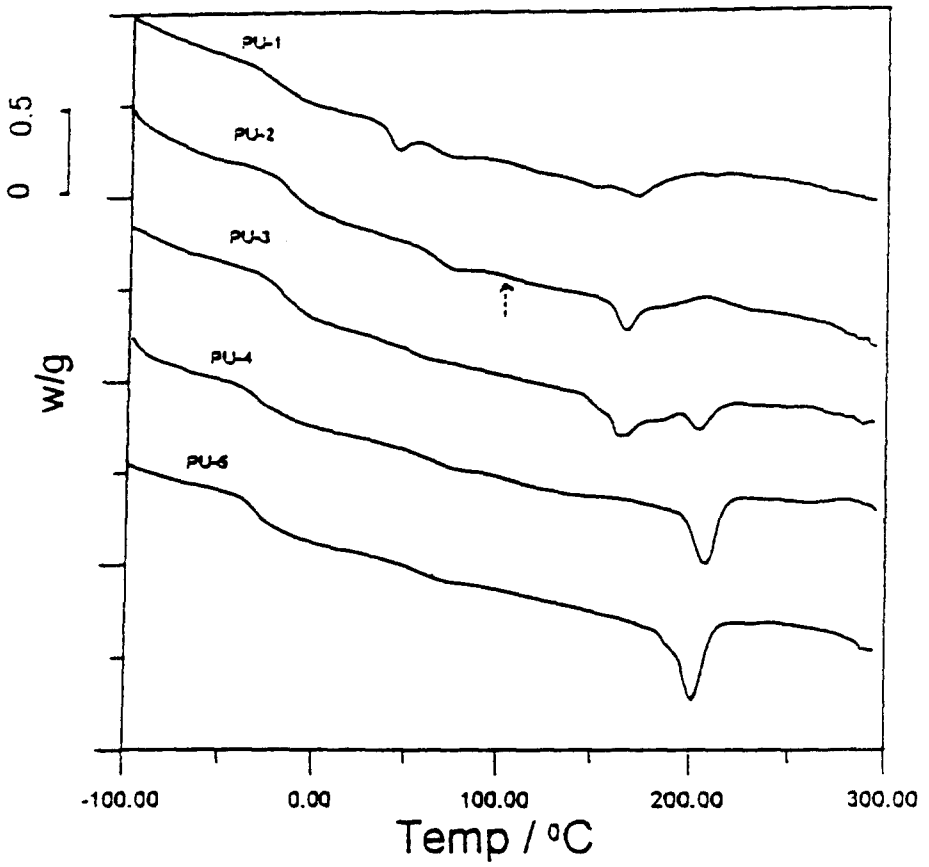

Figure 1 D.s.c. curves of polyurethanes annealed at room temperature then quenched to − 80°C

Table 3 D.s.c. data of polyurethanes annealed at room temperature

Polyurethane	PU-1	PU-2	PU-3	PU-4	PU-5
T_{g1}/°C	−23.4	−18.3	−21.5	−29.7	−28.1
T_{m1}(peak)/°C	42.9	—	—	—	—
ΔH_1/J g^{-1}	1.94	—	—	—	—
T_{m2}(I-peak)/°C	70.1	71.5	—	—	—
ΔH_2(I)/J g^{-1}	1.52	1.82	—	—	—
T_{g2}/°C	—	—	59.4	71.3	67.6
T_{m2}(II-a-peak)/°C	170.2	164.4	161.0	—	—
ΔH_2(II-a)/J g^{-1}	8.63	10.40	8.38	—	—
T_{m2}(II-b-peak)/°C	—	—	201.8	204.7	200.6
ΔH_2(II-b)/J g^{-1}	—	—	2.22	13.01	16.96

[a] The subscripts 1 and 2 correspond to soft and hard segments respectively

crystallization of one or both of the segments. The soft segment T_g is influenced by the restricted movement imposed at the hard segment junctions and at phase boundaries where the hard domain acts as a filler particle. The T_g of polyester-diol also depends on the molar ratio of 1,2-propanediol/hexanediol. The polyesters with a higher content of 1,2-propanediol have a lower soft segment T_{g1}. As indicated in *Figure 1* and *Table 3*, the glass transition temperature T_{g1} of soft segments decreased with the molar ratio of 1,2-propanediol/hexanediol. Thus PU-4 had the lowest T_{g1}, indicating the highest degree of the soft segment and hard segment phase segregation[33].

The second region of interest is that corresponding to crystalline melting of the soft segment (T_{m1}, between 40 and 50°C). T_{m1} and ΔH_1 of soft segments are indicators of soft segment crystallization[33]. The degree of crystallinity of polyester soft segments decreases as the concentration of polyester $-CH_3$ side chains (i.e. the molar ratio of 1,2-propanediol/hexanediol) increases. The experimental results revealed that only PU-1 had soft segment crystallization, indicating that the presence of $-CH_3$ side chains leads to a reduction of degree of soft segment crystallinity, i.e. less ordering of soft segments.

The third region of the d.s.c. results from the transition and endotherms that are associated with hard segment domains. The transition or endotherm in the region 55–75°C (T_{g2} or T_{m2}(I)), denoted Region-I, results from the dissociation of short-range order of the hard segments induced by room temperature annealing[34]. The transition (T_{g2}) and endotherm (T_{m2}(I)) around 60–75°C are respectively indicators of dispersion of hard segments in the soft segment phase and the short-range ordering of hard segment

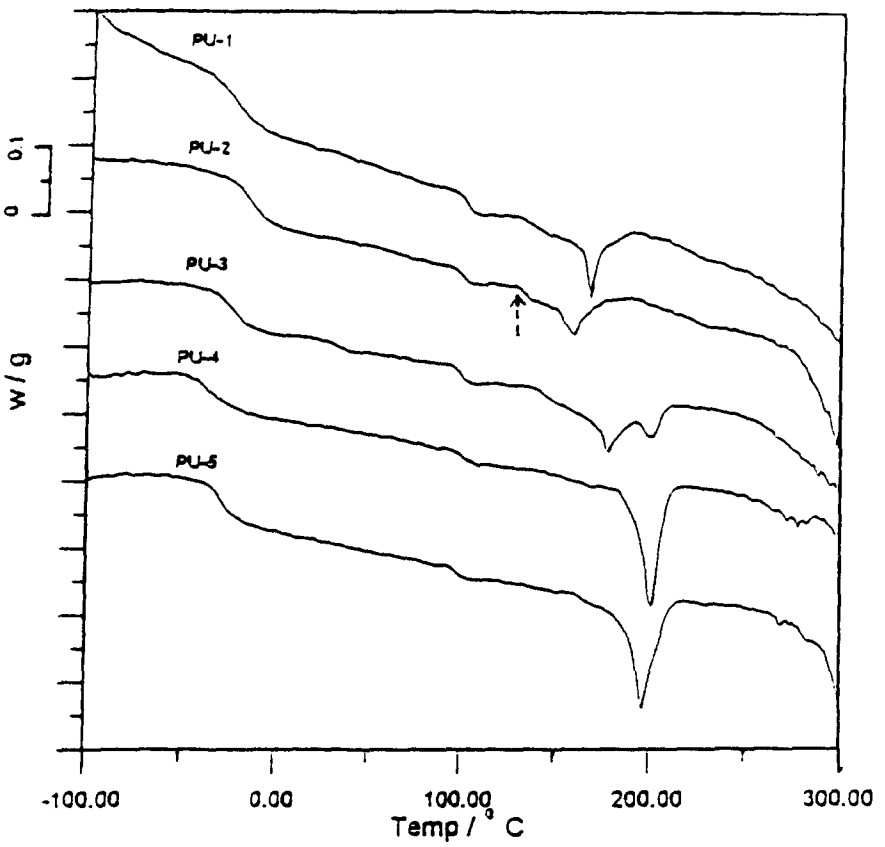

Figure 2 D.s.c. curves of polyurethanes annealed at 87°C for 1 h then quenched to −80°C

Table 4 D.s.c. data of polyurethanes annealed at 87°C

Polyurethane[a]	PU-1	PU-2	PU-3	PU-4	PU-5
T_{g1}/°C	−26.2	−19.86	−24.8	−36.5	−29.5
T_{m2}(I-peak)/°C	106.7	109.2	103.5	109.9	102.2
ΔH_2(I)/J g^{-1}	1.97	1.48	0.76	1.07	0.84
T_{m2}(II-a-peak)/°C	167.2	164.5	177.2	—	—
ΔH_2(II-a)/J g^{-1}	8.63	7.44	9.87	—	—
T_{m2}(II-b-peak)/°C	—	—	200.4	202.2	196.6
ΔH_2(II-b)/J g^{-1}	—	—	4.41	12.38	15.43

[a] The subscripts 1 and 2 correspond to soft and hard segments respectively

domains induced by annealing at room temperature[33]. Comparing the d.s.c. data of PU-1–PU-5, we found that PU-1 and PU-2 had melting endotherms around 55–75°C and PU-3–PU-5 had hard segment glass transitions around 55–80°C. In another study[35], we observed the thermal behaviour of these polyurethanes by using a penetrating mode thermal mechanical analysis. The slopes of the dimension change *versus* temperature for PU-1 and PU-2 were negative around 50–65°C, whilst the corresponding slopes of PU-3–PU-5 were positive around 60–100°C. Thus PU-1 and PU-2 had melting behaviour around 50–65°C, and PU-3 and PU-5 had glass transition behaviour around 60–100°C. The experimental results reveal that the introduction of $-CH_3$ side chains in polyesters leads to less short-range ordering of hard segments dispersed in the soft domain; no melting endotherm, but a glass transition around 55–75°C, was observed for PU-3–PU-5. The higher T_{g2} value of PU-4 than that of PU-5 could be due to the terminal secondary –OH group of polyester soft segments for PU-5 which resulted in less ordering of the hard segments and resulted in a higher degree of mixing of hard- and soft-segments.

The remaining regions of the d.s.c. thermal behaviour concerning the primary endotherms around 155–220°C (T_{m2}(II), Region II) correspond to the sequential melting/disruption of hard segment domains having different degrees of organization[33]. D.s.c. data revealed that the melting endotherm ΔH_2(II) of microcrystalline hard segments increased with the content of polyester $-CH_3$. As shown in *Figure 1*, the peak of the hard segment endotherm II was sharp and T_{m2}(II) was higher for PU-4 and PU-5, whereas the peak of hard segment endotherm II was broader and T_{m2}(II) was lower for PU-1 and PU-2. The glycol of polyester has a 1/1 molar ratio of hexanediol to 1,2-propanediol for PU-3. The d.s.c. results indicated two T_{m2}(II) endotherms. T_{m2}(II-a) corresponds to hexanediol-based polyester PU, whereas T_{m2}(II-b) corresponds to 1,2-propanediol-based polyester PU.

It is well known that morphological changes of segmental polyurethanes can be induced by annealing[10,33,34]. In

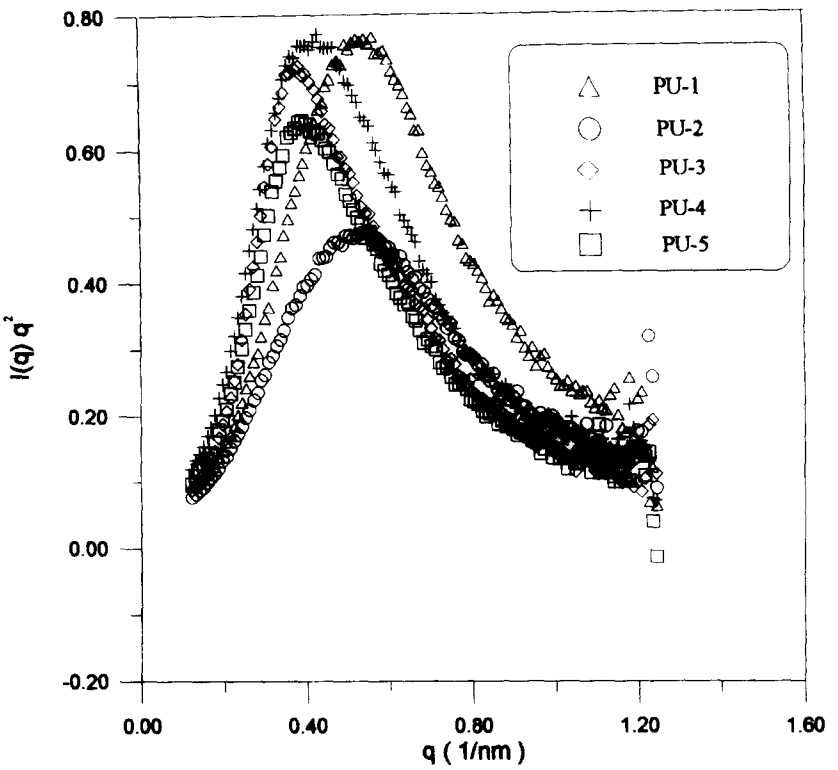

Figure 3 SAXS intensity profile Iq^2 *versus* q for polyurethanes annealed at room temperature for 1 week and measured at room temperature

general, annealing resulted in an endothermic peak at a temperature 20–50°C above that of the temperature of annealing. This annealing endotherm was ascribed to the disruption of an ordered segment structure resulting from the reorganization of less-ordered segments into more perfect arrangements upon annealing. The effect of polyester $-CH_3$ side-chain content on the phase segregation of hard and soft segments was also observed by d.s.c. at an annealing temperature of 87°C, which was slightly higher than the $T_{m2}(I)$ of the hard segments and about 40°C higher than the T_{m1} of the soft segments. Thus the soft segments of these polyurethanes were melted.

The d.s.c. curves of polyurethanes annealed at room temperature for 1 week followed by annealing at 87°C for 1 h and then quenched to −80°C are shown in *Figure 2*. The corresponding d.s.c. transitions and endotherms are listed in *Table 4*. Comparing the d.s.c. results of polyurethanes shown in *Tables 3 and 4*, we found that lower soft segment T_{g1} values were obtained for polyurethanes with the additional 1 h of annealing at 87°C, indicating the improvement of soft- and hard-segment segregation by annealing at 87°C for 1 h. However, the order of soft segment T_{g1} for polyurethanes annealed at 87°C was the same as those without annealing at 87°C, indicating that the effect of polyester $-CH_3$ side chains on phase segregation of polyurethanes was independent of the annealing temperature if the polyurethanes were annealed at a temperature between 25 and 87°C. The results of *Figure 2* and *Table 4* also revealed that no soft segment recrystallization was observed for any of the polyurethanes. The endotherm peak temperature $T_{m2}(I)$, induced by annealing at 87°C for 1 h, was around 103–110°C and was almost independent of the chemical composition of the soft segment. The heat of endotherm $\Delta H_2(I)$ value was highest for PU-1 and decreased as the polyester $-CH_3$ side-chain content increased. The d.s.c. results also showed that the melting endotherms of the hard segment microcrystalline regions ($T_{m2}(II)$ and $\Delta H_2(II)$) of PU-4 and PU-5 were almost not influenced by annealing at 87°C, indicating that the soft-segment viscosity had not decreased too much by increasing the annealing temperature from 25 to 87°C. However, the annealing at 87°C resulted in an increase in $\Delta H_2(II)$ of PU-1 and PU-3. Though the annealing at 87°C did not cause an increase in $\Delta H_2(II)$ for PU-2, upon careful investigation of the d.s.c. curves of PU-1 and PU-2 in *Figures 1 and 2*, we found that annealing for one more hour at 87°C led to a shift of the onset of melting endotherm-II from ~104°C to ~125°C (as designated by arrows in the d.s.c. curves) and a narrower distribution of endotherm-II for both PU-1 and PU-2. These results suggest that annealing at a temperature slightly higher than T_{g2} leads to a lower viscosity of soft segment and a higher mobility of hard segment molecules, thus improving the ordering of the hard segment lamellar structure for polyurethanes with lower content of polyester $-CH_3$ side chains (i.e. PU-1, PU-3). Summarizing the d.s.c. data, we may conclude that the introduction of polyester $-CH_3$ side chains improves the soft- and hard-segment segregation for polyurethanes annealed at a temperature between room temperature and 87°C which is slightly higher than $T_{m2}(I)$ of hard segments.

SAXS

The SAXS involves measurement of the scattering intensity as a function of the angle measured with respect to the direction of the incident X-ray beam. The scattering intensity arises due to local heterogeneities in the electron density of the material. For a two-phase system, the invariant quantity Q of overall mean-square electron density fluctuation is obtained by integrating $q^2I(q)$ over the range of scattering angles.

$$Q = \int_0^\infty q^2 I(q)\, dq \qquad (1)$$

Table 5 SAXS lamellar repeat distances of polyurethanes annealed at room temperature

Polyurethane	L (from invariant Q)/nm	L_{1D} (from γ_{1D})/nm	Q/arbitrary unit
PU-1	11.21	11.40	4.83
PU-2	11.59	11.90	3.49
PU-3	16.40	16.10	3.56
PU-4	14.62	14.10	4.43
PU-5	16.01	15.40	3.20

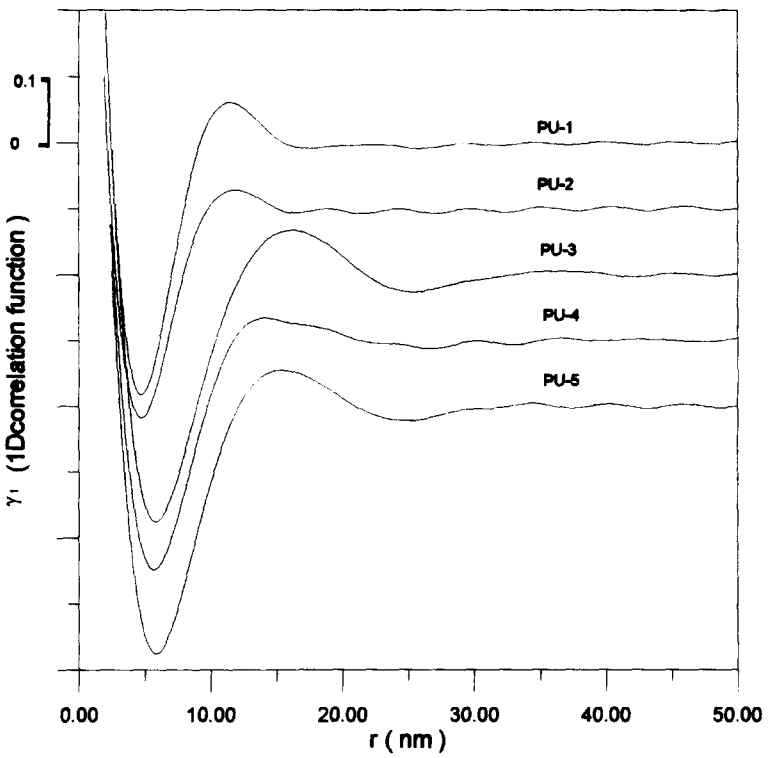

Figure 4 Correlation function $\gamma_1(r)$ from intensity profiles of polyurethanes annealed at room temperature for 1 week as shown in *Figure 3*

with

$$q = \frac{4\pi}{\lambda}\sin(\theta/2) \tag{2}$$

where q is the magnitude of scattering vector, θ is the scattering angle, λ is the wavelength, and $I(q)$ is the scattering intensity at q. The value of invariant Q describes the electron density fluctuation of polymer and is a good approximation to estimate the overall degree of phase separation in segmented polyurethanes. The Q values for polyurethanes annealed at 25°C are summarized in *Table 5*. As shown in *Table 5*, the Q value increased with polyester $-CH_3$ side-chain content for PU-2–PU-4. The higher Q value for PU-1 than PU-2 was due to the crystallization of polyester soft segments without $-CH_3$ side chains. The lower Q value of PU-5 than PU-4 could be due to the secondary –OH of the polyester soft segments of PU-5 leading to a lesser ordering of hard segments.

The inter-domain spacing L can be estimated from the q_m corresponding to the maximum of $I(q)q^2$ *versus* q curves (*Figure 3*) using Bragg's equation:

$$L = 2\pi/q_m \tag{3}$$

For systems with a lamellar structure, the one-dimensional correlation function $\gamma_1(r)$ will have a primary local maximum at a position r which corresponds to the inter-lamellar repeat distance L_{1D}. The one-dimensional correlation function is shown as follows:

$$\gamma_1(r) = \frac{1}{Q}\int_0^\infty q^2 I(q)\cos(qr)\,dq \tag{4}$$

Typical SAXS intensity profiles (Iq^2 *versus* q^2) for these polyurethanes annealed at room temperature are shown in *Figure 3*. These profiles all exhibited a single scattering maximum, indicative of the hard segment inter-domain repeat distance. The inter-domain repeat distance, L or L_{1D}, may be obtained from these data either by application of Bragg's law (equation (3)) or by correlation function analysis. The L values calculated from equation (3) for polyurethanes annealed at room temperature are listed in *Table 5*. Typical correlation functions $\gamma_1(r)$ for polyurethanes annealed at room temperature are shown in *Figure 4*. The periodicity is estimated from the position of the first subsidiary maximum in these correlation functions. The inter-domain repeat distances L_{1D} estimated from $\gamma_1(r)$ are also listed in *Table 5*.

The inter-domain repeat distance (L and L_{1D}) depends on the molecular length of the polyester soft segment, the number and size of hard segment lamellar crystalline particles and those of polyester crystalline particles. The L (or L_{1D}) increases with increasing polyester molecular chain length, and also with decreasing degree of polyester

Table 6 SAXS interfacial parameters for diffuse boundary thickness of polyurethanes annealed and measured at room temperature

Polyurethane	$\langle\eta^2\rangle \times 10^{18}/\text{cm}^{-4}$	$K_p \times 10^{-29}/\text{cm}^{-5}$	σ/nm	l_p/nm	I_b/cm^{-1}
PU-1	3.70	3.34	0.64	4.98	0.0399
PU-2	4.60	2.96	0.74	4.09	0.0213
PU-3	9.90	2.07	0.80	3.12	0.0388
PU-4	12.59	2.18	0.61	3.23	0.0269
PU-5	8.59	1.94	0.85	3.49	0.0544

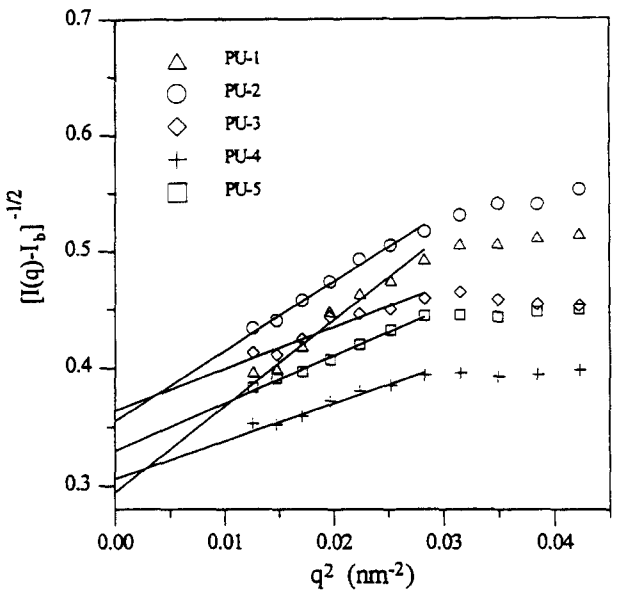

Figure 5 Plots of $[I(q) - I_b]^{-1/2}$ *versus* q^2 at $q \rightarrow 0$ for polyurethanes annealed at room temperature; full lines are simulated results

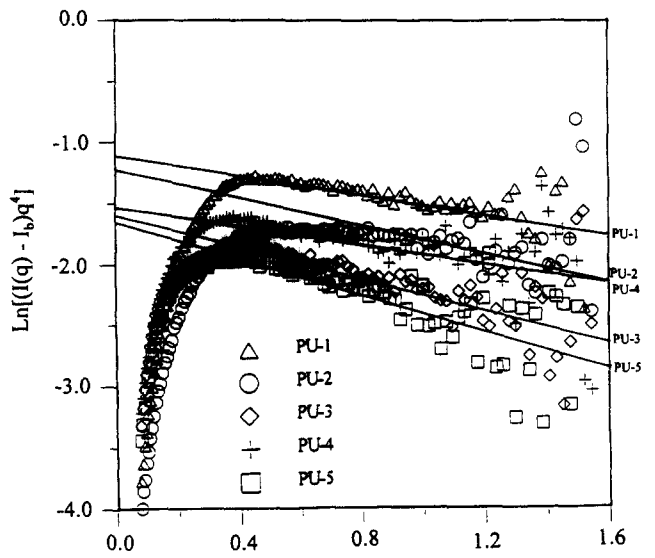

Figure 6 Plots of $\ln\{[I(q) - I_b]q^4\}$ *versus* q^2 at $q \rightarrow \infty$ for polyurethanes annealed at room temperature; full lines are simulated results

crystallinity. For a fixed degree of soft- and hard-crystallinity (i.e. the sum of ΔH_1 and ΔH_2 of d.s.c. data is constant), L (or L_{1D}) decreases with increasing number of crystalline particles (or with decreasing size of crystalline domain, i.e. decreasing T_{m1} and T_{m2}). The morphologies of these block polyurethanes based on the results of d.s.c. and SAXS will be discussed later.

The range of inhomogeneity l_p is a measure of the average size or distance for which all the inhomogeneities in the material exist. According to Debye–Bueche theory[36], the l_p value can be obtained by applying the following equation to $q \rightarrow 0$:

$$\lim_{q\to 0} I(q) = \lim_{q\to 0} \frac{8\pi\langle\eta^2\rangle l_p^3}{(1+l_p^2q^2)^2} + I_b \tag{5}$$

where $\langle\eta^2\rangle$ is the mean-square electron density fluctuation and I_b the background intensity.

Extrapolation of the scattering intensity to an infinite scattering vector allows us to calculate Porod's law constant K_p[37,38]:

$$\lim_{q\to\infty} I(q) = \lim_{q\to\infty} (K_p/q^4)\exp(-\sigma^2q^2) + I_b \tag{6}$$

where σ is the interfacial boundary thickness parameter. Porod's law constant K_p is related to the interface surface-to-volume ratio S/V by the relation

$$K_p = 2\pi i_e\langle\eta^2\rangle(S/V) \tag{7}$$

where i_e is the Thompson scattering factor for a single electron. The value of the Porod constant K_p can be used to determine S/V using equation (7). An equivalent thickness E for an inter-phase gradient is given by

$$E = 12^{1/2}\sigma \tag{8}$$

Rearranging equation (5), we obtain

$$[I(q) - I_b]^{-1/2} = (8\pi\langle\eta^2\rangle l_p^3)^{-1/2}(1 + l_p^2q^2) \tag{9}$$

The values of $\langle\eta^2\rangle$ and l_p can be obtained from the slope and intercept of a plot of the left-hand side of equation (9) against q^2 as q $\rightarrow$ 0. Similarly, rearranging equation (6), we obtain

$$\ln\{[I(q) - I_b]q^4\} = \ln K_p - \sigma^2q^2 \tag{10}$$

The values of σ and K_p can be obtained from the slope and intercept respectively of a plot of the left-hand side of equation (10) against q^2 as $q \rightarrow \infty$.

Since the $I(q)$ data at high q were noisy, it was hard to obtain I_b values. In this study, we simulated the $I(q)$ data at $q \rightarrow \infty$ by using equations (5) and (6) with a non-linear least squares method. By adjusting the difference between the I_b data obtained from equation (5) and equation (6) to be less than 3%, we obtained parameters $\langle\eta^2\rangle$ and l_p (from equation (5)) and K_p and σ (from equation (6)) for polyurethanes annealed at room temperature; these are summarized in *Table 6*. Typical plots of equations (9) and (10) of SAXS data at $q \rightarrow 0$ and $q \rightarrow \infty$ respectively, together with their simulated results, are shown in *Figures 5 and 6* respectively for polyurethanes annealed at room temperature. Comparing the SAXS data of PU-1–PU-4, we found that the interfacial boundary thickness increased with increasing polyester $-CH_3$ side-chain content from PU-1

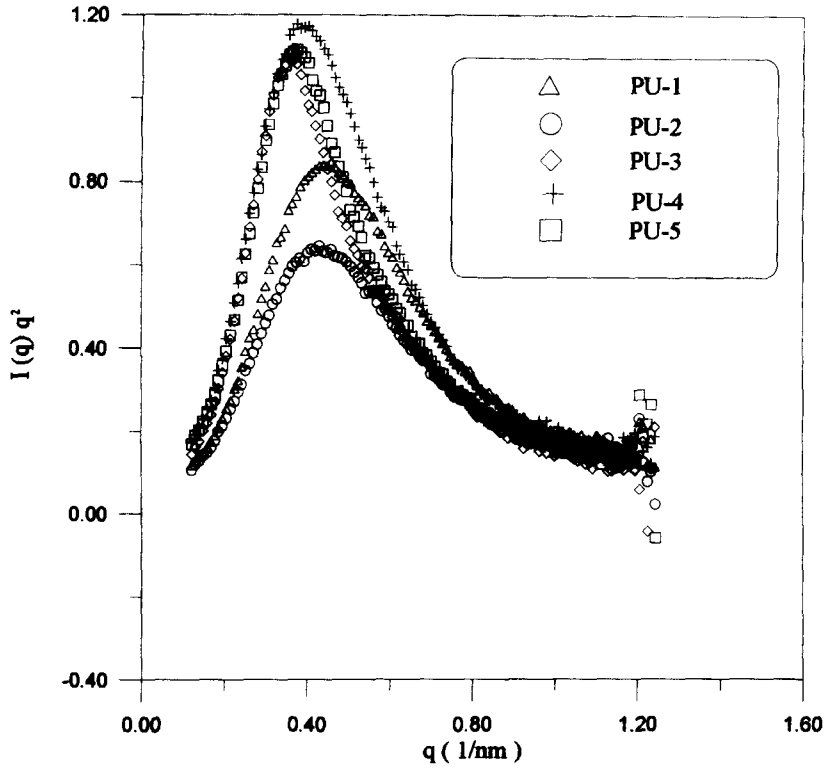

Figure 7 SAXS intensity profile Iq^2 *versus* q for polyurethanes annealed at 87°C for 1 h and measured at 87°C

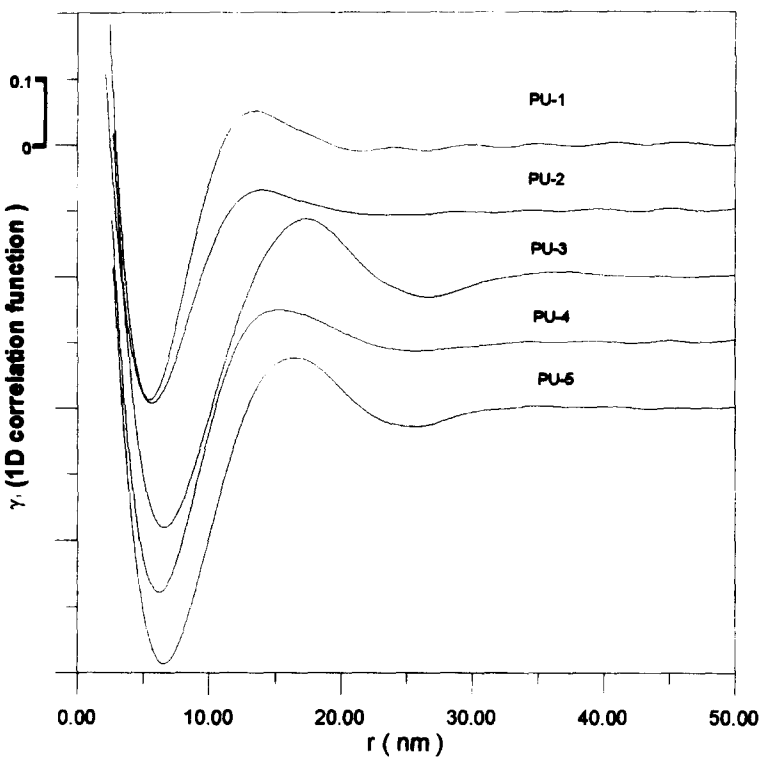

Figure 8 Correlation function $\gamma_1(r)$ obtained from intensity profiles of polyurethanes annealed at 87°C for 1 h and measured at 87°C as shown in *Figure 5*

to PU-3, and decreased with increasing polyester $-CH_3$ side-chain content from PU-3 to PU-4. The increase of interfacial boundary thickness from PU-1 to PU-3 was due to the decrease of soft segment crystallinity with increasing polyester $-CH_3$ side-chain content. However, the decreasing of interfacial lamellar thickness from PU-3 to PU-4 was due to the increase in the long-range ordering of the hard segment lamellar domain (see *Table 3*, the ΔH_2(II) and T_{m2}(II) of PU-4 were larger and higher than those of PU-3). These results were due to a large lamellar thickness reducing the diffuse boundary thickness of the micro-domains. A thicker interface boundary requires dissolution of longer hard segments into the soft micro-phase. The larger interfacial boundary thickness for PU-5 than for PU-4

Table 7 SAXS lamellar repeat distances for polyurethanes annealed and measured at 87°C

Polyurethane	L (from Iq^2)/nm	L_{1D} (from γ_{1D})/nm	Q/arbitrary unit
PU-1	13.72	13.40	4.57
PU-2	14.62	13.90	4.30
PU-3	17.69	17.40	4.57
PU-4	16.81	15.30	5.88
PU-5	16.81	16.40	4.82

Table 8 SAXS interfacial parameters for diffuse boundary thickness of polyurethanes annealed and measured at 87°C

Polyurethane	$\langle\eta^2\rangle \times 10^{18}/\text{cm}^{-4}$	$K_p \times 10^{-29}/\text{cm}^{-5}$	σ/nm	l_p/nm	I_b/cm^{-1}
PU-1	10.24	2.92	0.81	3.46	0.0399
PU-2	10.42	2.66	0.76	3.33	0.0213
PU-3	24.34	2.41	0.90	2.35	0.0388
PU-4	24.52	2.64	0.70	2.86	0.0269
PU-5	21.92	2.28	0.83	2.97	0.0544

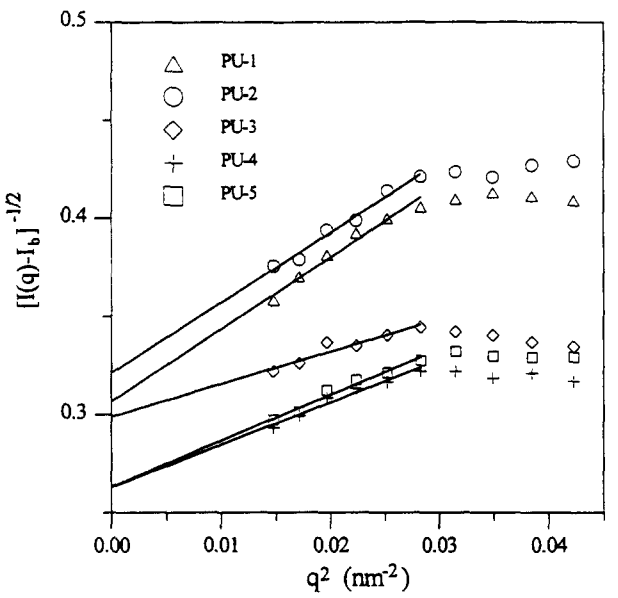

Figure 9 Plots of $[I(q) - I_b]^{-1/2}$ *versus* q^2 at $q \rightarrow 0$ for polyurethanes annealed at 87°C; full lines are simulated results

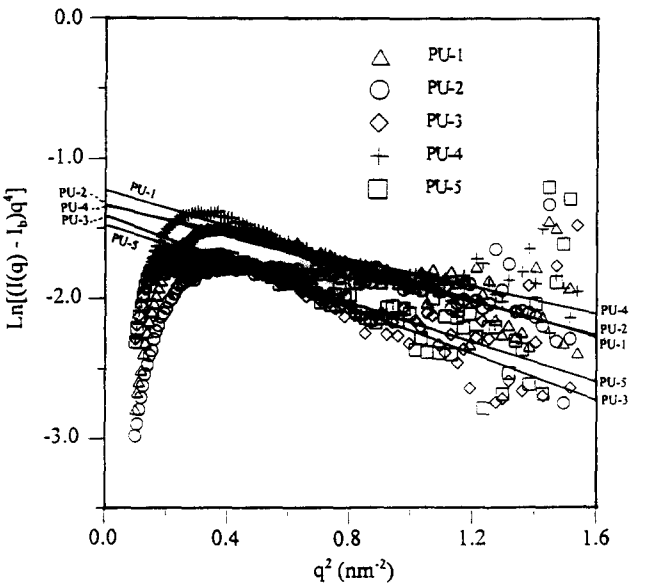

Figure 10 Plots of $\ln[[I(q) - I_b]q^4]$ *versus* q^2 at $q \rightarrow \infty$ for polyurethanes annealed at 87°C; full lines are simulated results

was due to the polyester terminal secondary –OH group of PU-5 which resulted in less ordering of the hard segments.

The morphology of the polyurethanes annealed at room temperature for 1 week followed by annealing at 87°C for 1 h was also observed at 87°C by SAXS. The SAXS intensity $I(q)q^2$ *versus* q profiles and correlation functions $\gamma_1(r)$ are shown in *Figures 7 and 8* respectively. The lamellar repeat distance obtained from invariant Q and γ_{1D} are summarized in *Table 7*. The plots of equations (9) and (10) for SAXS data, together with the simulated results, are shown in *Figures 9 and 10* respectively; the simulated values of $\langle\eta^2\rangle$, l_p, K_p, σ and I_b are summarized in *Table 8*. Comparing the data of *Table 5* and *Table 7*, we found that the lamellar repeat distance L or L_{1D} was larger for PU samples annealed and measured at 87°C, indicating a shift upward due to thermal expansion of the two phases. A comparison of the data of *Table 6* and *Table 8* also suggested that the interfacial boundary thickness was larger and the inhomogeneous length was shorter for PU samples annealed and measured at 87°C, suggesting a higher degree of mixing of hard- and soft-segments at higher annealing temperature. However, the sequence of L or L_{1D} and the sequences of K_p, σ and l_p for PU-1–PU-5 were not changed after annealing at 87°C for 1 h.

From the results of d.s.c. and SAXS observations, it is obvious that the content of polyester $-CH_3$ side-chain has a strong influence on the morphology of polyurethanes annealed at a temperature between 25 and 87°C. The polyurethane with a higher polyester $-CH_3$ side-chain content caused a lower viscosity of the soft segment and a higher mobility of the hard segments within the soft domain. Increasing the mobility of the hard segments resulted in an increase in the aggregation of the hard segments and an increase in the soft- and hard-segment segregation during annealing.

The morphology of these polyurethanes is pictured in *Figure 11* with the hatched regions denoting the ordering in the hard segment crystalline domain, the cross-hatched regions denoting the polyester crystalline domain and the coiled lines as the amorphous polyester and urethane molecules. Comparing the values of L and L_{1D}

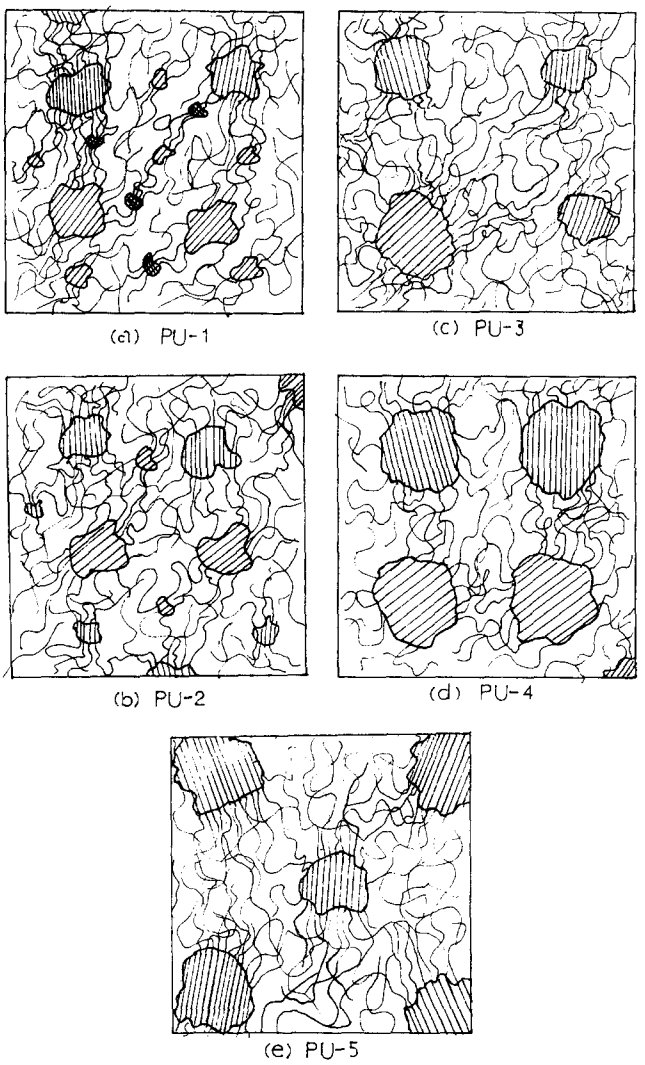

Figure 11 Morphology of polyurethanes: ( ) amorphous polyester and urethane; ( ) polyester crystalline; ( ) hard segment lamellar domain. (a) PU-1; (b) PU-2; (c) PU-3; (d) PU-4; (e) PU-5

for PU-1–PU-3 (*Tables 5, and 7*), we find that inter-domain repeat distance increased with polyester $-CH_3$ side-chain content. From d.s.c. data (*Table 3* and *Figure 1*), we know that there were T_{m1} and T_{m2}(I) d.s.c. endotherms for PU-1, indicating crystallization of polyester soft segments and small hard segment crystalline particles dispersed in the amorphous polyester domain. As shown in *Figure 11a*, the large hatched regions were the long-range ordering hard segment domains (T_{m2}(II) of d.s.c.), the small hatched regions were the short-range ordering of the hard segment domains (T_{m2}(I) of d.s.c.), and the cross-hatched regions were the small polyester crystalline particles (T_{m1} of d.s.c.) dispersed in the amorphous soft domain. As we introduced the $-CH_3$ side chains in the polyester soft segment, the crystallization of the polyester disappeared, and only leaving the small hard segment crystalline particles dispersed in the amorphous soft domain. Thus the L and L_{1D} of PU-2 were longer than those of PU-1 (*Figure 11b*). As the content of polyester side chains was increased, the mobility of the hard segments was increased due to the lower viscosity and higher free volume of the soft domain. Thus more and more hard segment molecules aggregated and less small hard segment particles dispersed in the amorphous soft domain, leading to a longer L (or L_{1D}). As shown in *Figure 11c*, the inter-domain repeat distance of PU-3 was longer than that of PU-2. The other reason for the longer L (or L_{1D}) for PU-3 than for PU-2 is the higher polyester molecular weight of PU-3, which resulted in longer polyester coiled lines in *Figure 11c* than in *Figure 11b*. In *Figure 11c*, two different sizes of hard domain are shown. The smaller domains correspond to the d.s.c. endotherm T_{m2}(II-a), whereas the larger domains correspond to the d.s.c. endotherm of T_{m2}(II-b). Inspecting the d.s.c. data of PU-3–PU-5, we found that T_{g2}, rather than the short-range ordering hard segment melting endotherm T_{m2}(I), was observed in these polyurethanes. Owing to the higher content of polyester $-CH_3$ side chains, the free volume of the amorphous soft domains was larger for PU-4 than that for PU-3, leading to the higher mobility of the hard segment molecules and a larger hard segment aggregation of PU-4. Thus a thicker hard segment lamellar structure was obtained for PU-4 than for PU-3, leading to a higher hard segment endotherm T_{m2}(II) and a shorter repeat distance (L and L_{1D}) for PU-4 than for PU-3 (*Figure 11d*). The lower polyester molecular weight of PU-4 was also the reason for PU-4 having a shorter L (or L_{1D}) than PU-3. Comparing the morphology of PU-4 and PU-5, though the terminal secondary –OH group of polyesters caused a lesser

ordering of hard segments, and hence, led to thinner lamellar hard segment domains and a slight increase in the number of hard segment crystalline particles for PU-5 (PU-5 has a lower T_{m2}(II) and a larger ΔH_2(II) than PU-4); however, owing to the longer polyester chain length, PU-5 has a longer inter-lamellar repeat distance (L and L_{1D}) (*Figure 11e*).

CONCLUSION

A combination of d.s.c. and SAXS has been used to characterize the multiphase structure of polyurethanes with various contents of polyester $-CH_3$ side chains. The introduction of $-CH_3$ side chains in the polyester segment results in an increase in free volume, a decrease in viscosity and less ordering of the soft segments. The mobility of the hard segments and the viscosity of the system are two important factors controlling the phase-separation process[15]. When the polyurethane samples were annealed at 175°C for 10 min and then annealed at a temperature between room temperature and 87°C (near the T_g of the hard segments), the mobility of the hard segments are found to depend strongly on the viscosity of the polyester soft segment during cooling of the samples. The d.s.c. and SAXS results revealed that better phase separation and larger micro-crystalline hard segment domains were obtained with increasing content of polyester $-CH_3$ side chains.

REFERENCES

1. Cooper, S. L. and Tobolsky, A. V., *J. Appl. Polym. Soc.*, 1966, **10**, 1837.
2. Kwei, T. K., *J. Appl. Polym. Sci.*, 1982, **27**, 2891.
3. Huh, D. S. and Cooper, S. C., *Polym. Eng. Sci.*, 1971, **11**, 369.
4. Wilkes, C. E. and Yusek, C. S., *J. Macromol. Sci. Phys. B*, 1973, **7**, 157.
5. Seefried, G. G. Jr., Koleske, J. V. and Critchfield, F. R., *J. Appl. Polym. Sci.*, 1975, **19**, 2493.
6. Seefried, G. G. Jr., Koleske, J. V. and Critchfield, F. R., *J. Appl. Polym. Sci.*, 1975, **19**, 3185.
7. Miller, G. W. and Saunders, J. H., *J. Polym. Sci. A*, 1970, **18**, 1923.
8. Abouzahr, S. and Wilkes, G. L., *J. Appl. Polym. Sci.*, 1984, **29**, 2695.
9. Miller, J. A., Lin, S. B., Hwang, K. K. S., Wu, K. S., Gibson, P. E. and Cooper, S. L., *Macromolecules*, 1985, **18**, 32.
10. Seymour, R. W. and Cooper, S. L., *Macromolecules*, 1973, **6**, 48.
11. Koberstein, J. T. and Russell, T. P., *Macromolecules*, 1986, **19**, 714.
12. Koberstein, J. T. and Galambos, A. G., *Macromolecules*, 1992, **25**, 5618.
13. Koberstein, J. T., Galambos, A. G. and Leung, L. M., *Macromolecules*, 1992, **25**, 6195.
14. Koberstein, J. T. and Leung, L. M., *Macromolecules*, 1992, **25**, 6205.
15. Li, Y., Gao, T. and Chu, B., *Macromolecules*, 1992, **25**, 1737.
16. Li, Y., Gao, T., Liu, J., Linliu, K., Desper, K. and Chu, B., *Macromolecules*, 1992, **25**, 7365.
17. Li, Y., Liu, J., Yang, H., Ma, D. and Chu, B., *J. Polym. Sci. Polym. Phys. Ed.*, 1993, **31**, 853.
18. Li, Y., Kang, W., Staffer, J. O. and Chu, B., *Macromolecules*, 1994, **27**, 612.
19. Goddar, R. J. and Cooper, S. L., *J. Polym. Sci. Polym. Phys. Ed.*, 1994, **32**, 1557.
20. Grady, B. P., O'Connell, E. M., Yang, C. Z. and Cooper, S. L., *J. Polym. Sci. Polym. Phys. Ed.*, 1994, **32**, 2357.
21. Goddar, R. J. and Cooper, S. L., *Macromolecules*, 1995, **28**, 1401.
22. Paik Sung, C. S., Hu, C. B. and Wu, C. S., *Macromolecules*, 1980, **13**, 111.
23. Miller, J. A. and Cooper, S. L., *J. Polym. Sci. Polym. Phys. Ed.*, 1985, **23**, 1065.
24. Leung, L. M. and Koberstein, J. T., *Macromolecules*, 1986, **19**, 706.
25. Koberstein, J. T. and Gancarz, I., *J. Polym. Sci. Polym. Phys. Ed.*, 1986, **24**, 2487.
26. West, J. C. and Cooper, S. L., *J. Polym. Sci. Polym. Symp.*, 1977, **60**, 27.
27. Coleman, M. M., Lee, K. H., Skrovanek, D. J. and Painter, D. C., *Macromolecules*, 1986, **19**, 2149.
28. Goddar, R. J. and Cooper, S. L., *Macromolecules*, 1995, **28**, 1390.
29. Tao, H. J., Meuse, G. W., Yang, X., MacKnight, W. J. and Hsu, S. L., *Macromolecules*, 1994, **27**, 7146.
30. Gower, L. A. and Lyman, D. J., *J. Polym. Sci. Polym. Chem. Ed.*, 1995, **33**, 2257.
31. Wilkes, G. L., Samuel, S. L. and Crystal, R. G., *J. Macromol. Sci. Phys. B*, 1974, **10**, 203.
32. Foka, J. and Janik, H., *Polym. Eng. Sci.*, 1989, **29**, 113.
33. Hesketh, T. R., Van Bogart, J. W. C. and Cooper, S. L., *Polym. Eng. Sci.*, 1980, **20**, 190.
34. Wang, C. B. and Cooper, S. L., *Macromolecules*, 1983, **16**, 775.
35. Chen, W. C., Chen, Y. S., Yu, T. L. and Tseng, Y. H., *J. Macromol. Sci. Pure Appl. Polym. Chem.* (in press).
36. Debye, P. and Bueche, A. M., *J. Appl. Phys.*, 1949, **20**, 5518.
37. Porod, G., *Kolloid Z. Z. Polym.*, 1951, **124**, 83.
38. Ruland, W., *J. Appl. Crystallogr.*, 1971, **4**, 70.